iScience

CellPress
OPEN ACCESS

Article

Dopamine induces functional extracellular traps in microglia

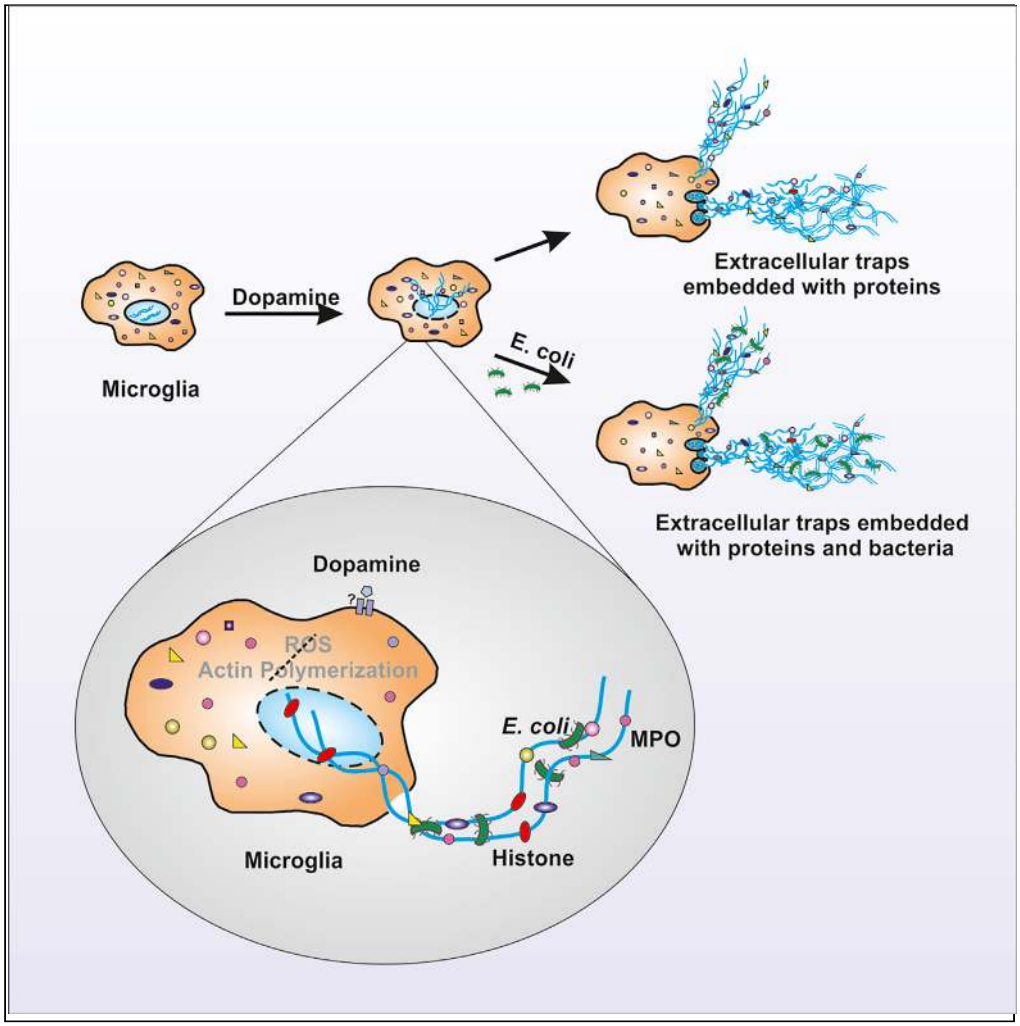

Ishan Agrawal, Nidhi Sharma, Shivanjali Saxena, ..., Sridhar Epari, Tejpal Gupta, Sushmita Jha

sushmitajha@iitj.ac.in

HIGHLIGHTS

Dopamine induces ETs in BV2 microglia and primary adult human microglia

Induced traps are independent of ROS, cell death, and actin polymerization

Microglia ETs are functional and can trap *E. coli*

Microglia ETs are also present in *Glioblastoma multiforme*

Agrawal et al., iScience *24*, 101968
January 22, 2021
https://doi.org/10.1016/j.isci.2020.101968

iScience

CellPress
OPEN ACCESS

Article

Dopamine induces functional extracellular traps in microglia

Ishan Agrawal,[1] Nidhi Sharma,[1,7] Shivanjali Saxena,[1] S. Arvind,[1] Debayani Chakraborty,[1] Debarati Bhunia Chakraborty,[2] Deepak Jha,[3] Surajit Ghatak,[4] Sridhar Epari,[5] Tejpal Gupta,[6] and Sushmita Jha[1,8,*]

SUMMARY

Dopamine (DA) plays many roles in the brain, especially in movement, motivation, and reinforcement of behavior; however, its role in regulating innate immunity is not clear. Here, we show that DA can induce DNA-based extracellular traps in primary, adult, human microglia and BV2 microglia cell line. These DNA-based extracellular traps are formed independent of reactive oxygen species, actin polymerization, and cell death. These traps are functional and capture fluorescein (FITC)-tagged *Escherichia coli* even when reactive oxygen species production or actin polymerization is inhibited. We show that microglial extracellular traps are present in *Glioblastoma multiforme*. This is crucial because *Glioblastoma multiforme* cells are known to secrete DA. Our findings demonstrate that DA plays a significant role in sterile neuro-inflammation by inducing microglia extracellular traps.

INTRODUCTION

In 2004, Zychklinsky et al. discovered that neutrophils can control the spread of pathogens by forming extracellular traps (ETs), also referred to as neutrophil extracellular traps (NETs). ETs are composed of nuclear or mitochondrial DNA (Brinkmann et al., 2004; Lood et al., 2016; Pocock and Kettenmann, 2007). ETs are decorated with multiple antimicrobial proteins like myeloperoxidase (MPO) and neutrophil elastase (NE) (Delgado-Rizo et al., 2017; Dwyer et al., 2014; Papayannopoulos, 2017) and are capable of trapping and killing bacteria (Brinkmann et al., 2004), fungi (Urban et al., 2006), parasites (Abi Abdallah et al., 2012), and viruses (Saitoh et al., 2012) It is now known that innate immune cells such as monocytes (Webster et al., 2010), macrophages (Chow et al., 2010), eosinophils ((Gupta et al., 2010)Yousefi et al., 2008), basophils (Morshed et al., 2014; Schorn et al., 2012), and mast cells (Möllerherm et al., 2016) can also form ETs.

Two mechanisms are proposed for NETs formation (NETosis): suicidal or lytic NETosis and vital or non-lytic NETosis (Fuchs et al., 2007; Papayannopoulos, 2017; Pilsczek et al., 2010; Yipp et al., 2012; Yousefi et al., 2019). In lytic NETosis, decondensed chromatin is released with the permeabilization of nuclear envelop and cell membrane leading to immediate cell death (Fuchs et al., 2010; Papayannopoulos, 2017). In non-lytic NETosis, decondensed chromatin is released in vesicles along with granules containing antimicrobial proteins without compromising the cell membrane and cells continue to function normally (Papayannopoulos, 2017; Yipp et al., 2012). Yousefi et al. first reported that viable neutrophils can produce NETs composed of mitochondrial DNA rather than nuclear DNA (Yousefi et al., 2009). Lytic NETosis is most studied and is reactive oxygen species (ROS) dependent (Fuchs et al., 2010; Papayannopoulos, 2017). The precise mechanism behind NETosis is still not known and is a topic of intense research. Stimuli-like PMA (phorbol 12-myristate 13-acetate), LPSs (lipopolysaccharides), platelets, granulocyte-macrophage colony-stimulating factor, oxidized low-density lipoprotein, and statins induce ETs (Caudrillier et al., 2012; Delgado-Rizo et al., 2017; Wang et al., 2019; Chow et al., 2010). Pathologic conditions such as hyperglycemia impair the ability of neutrophils to form NETs and reduce their antimicrobial properties (Joshi et al., 2013).

ETs play an important role in immune surveillance and pathogen clearance, but their persistence post infection makes them inflammatory and harmful (Kolaczkowska et al., 2015; Hakkim et al., 2010; Papayannopoulos, 2017; Pocock and Kettenmann, 2007; Wright et al., 2016). ETs contribute to tissue damage

[1]Department of Bioscience and Bioengineering, Indian Institute of Technology Jodhpur, Jodhpur, Rajasthan 342037, India

[2]Department of Computer Science and Engineering, Indian Institute of Technology Jodhpur, Jodhpur, Rajasthan 342037, India

[3]Department of Neurosurgery, All India Institute of Medical Sciences Jodhpur, Jodhpur, 342005 Rajasthan, India

[4]Department of Anatomy, All India Institute of Medical Sciences Jodhpur, Jodhpur, 342005 Rajasthan, India

[5]Department of Pathology, Tata Memorial Hospital, Mumbai, 400012 Maharashtra, India

[6]Department of Radiation Oncology, Tata Memorial Hospital, Mumbai, 400012, Maharashtra, India

[7]Karolinska Institute and Scilifelab, Stockholm, Sweden

[8]Lead contact

*Correspondence: sushmitajha@iitj.ac.in

https://doi.org/10.1016/j.isci.2020.101968

(Czaikoski et al., 2016; Saffarzadeh et al., 2012; Villanueva et al., 2011), vaso-occlusion (Fuchs et al., 2010; Martinod et al., 2013), sterile inflammation (Warnatsch et al., 2015), cancer (Cedervall et al., 2015; Demers et al., 2012; Guglietta et al., 2016), rheumatoid arthritis (Khandpur et al., 2013), and systemic lupus erythematosus (Garcia-Romo et al., 2011; Yu and Su, 2013). Calcium-phosphate-based mineralo-organic particles, some of which are spontaneously generated in the body, induce NETs that leads to inflammation through high-mobility group protein B1 (Peng et al., 2017). It is critical to understand the regulation of formation and disassembly of ETs for therapeutic interventions.

Innate immune cells form ETs; macrophages forming ETs are actively studied. Human peripheral blood monocytes (Jönsson et al., 2013; Halder et al., 2016), human monocyte-derived macrophages (Wong and Jacobs, 2013), human alveolar macrophages (King et al., 2015), THP-1 monocytic cell line (Shen et al., 2016), murine peritoneal macrophages (Chow et al., 2010), and rat macrophages (Bryukhin and Shopova, 2015) form ETs, referred to as macrophage extracellular traps (Doster et al., 2017). Until recently, ET formation by microglia was not reported (Wang et al., 2019). Microglia are resident myeloid cells of the central nervous system (CNS). They play critical role in clearing debris and maintaining homeostasis in the CNS (Li and Barres, 2018). These roles of microglia are regulated by multiple factors including neurotransmitters (Pocock and Kettenmann, 2007; Fan et al., 2018; Yoshioka et al., 2016). Dopamine (DA) is one of the key neurotransmitters in the brain. It controls a variety of functions including locomotor activities, emotion, and cognition (Beninger, 1983; Ferreri et al., 2019; Ott and Nieder, 2019). DA is also important for immunity within the CNS and in the body (Fan et al., 2018; Arreola et al., 2016). Recently, Caragher et al. reported that glioblastoma (GBM) cells express dopamine receptor 2 (DR2) and can synthesize and secrete DA (Caragher et al., 2019). This affects GBM metabolism and may enhance tumor growth. Activation of DR2 increases spheroid forming capacity of GBM cells (Caragher et al., 2019; Weissenrieder et al., 2019). These findings indicate a possible role of DA in the regulation of GBM.

Based on these observations, we investigated whether DA can induce ETs in BV2 microglia cell line and primary adult human microglia. We explored the basic mechanism of microglia ET formation, functionality of these traps, and their presence in GBM.

RESULTS

Dopamine induces formation of extracellular traps in microglia

We started with examining whether DA induces ET formation in BV2 microglia cell line. We treated the cells with different concentrations of DA for 24 hours. All the concentrations of DA induced traps like structures in BV2 microglia cell as visualized by phase contrast microscopy (Figure 1A). We used 250μM of DA for further experiments. ETs are composed of decondensed chromatin and hence they are stained by (4′,6-Diamidine-2′-phenylindole dihydrochloride) DAPI. Antimicrobial protein MPO is also embedded on ETs. We stained the DA-induced trap-like structures with DAPI (Figures 1B and 1C) and MPO that confirmed their identity as ETs. We further quantified the presence of ETs in the culture supernatant by digesting them with DNase I which showed that DA was inducing ETs in BV2 microglia cell line (Figure 1D).

Extracellular traps are being formed independent of cell death

We next performed (Methylthiazolyldiphenyl-tetrazolium bromide) MTT assays to determine whether ETs are induced by lytic ETosis or vital ETosis (Figure 2). DA did not cause significant cell death at any concentration. This confirmed that DA-induced BV2 microglia cells are following vital ETosis. To investigate the mechanism of ET formation in BV2 cells, we have used NAC (N-acetyl-L-cysteine), an antioxidant, and cytochalasin D (CytoD), an actin polymerization inhibitor, along with DA in our experiments. We checked the cytotoxicity of NAC and CytoD along with DA on BV2 microglia cells. NAC and DA did not cause significant cell death while CytoD and DA were toxic to cells.

Microglia form extracellular traps in an ROS-independent manner

Formation of ETs is ROS dependent and/or independent (Papayannopoulos, 2017). To examine which pathway contributes to ET formation in BV2 microglia, we inhibited ROS production by pretreating the cells with NAC and confirmed the inhibition by dichlorofluorescin diacetate (Figure 3A). We observed that DA itself did not induce ROS; hence, NAC did not have significant effect on the level of ROS. This result suggests that DA induces ETs in an ROS-independent manner. To confirm this finding, we treated ROS inhibited BV2 cells with DA and observed ET formation. Inhibition of ROS did not inhibit the formation of

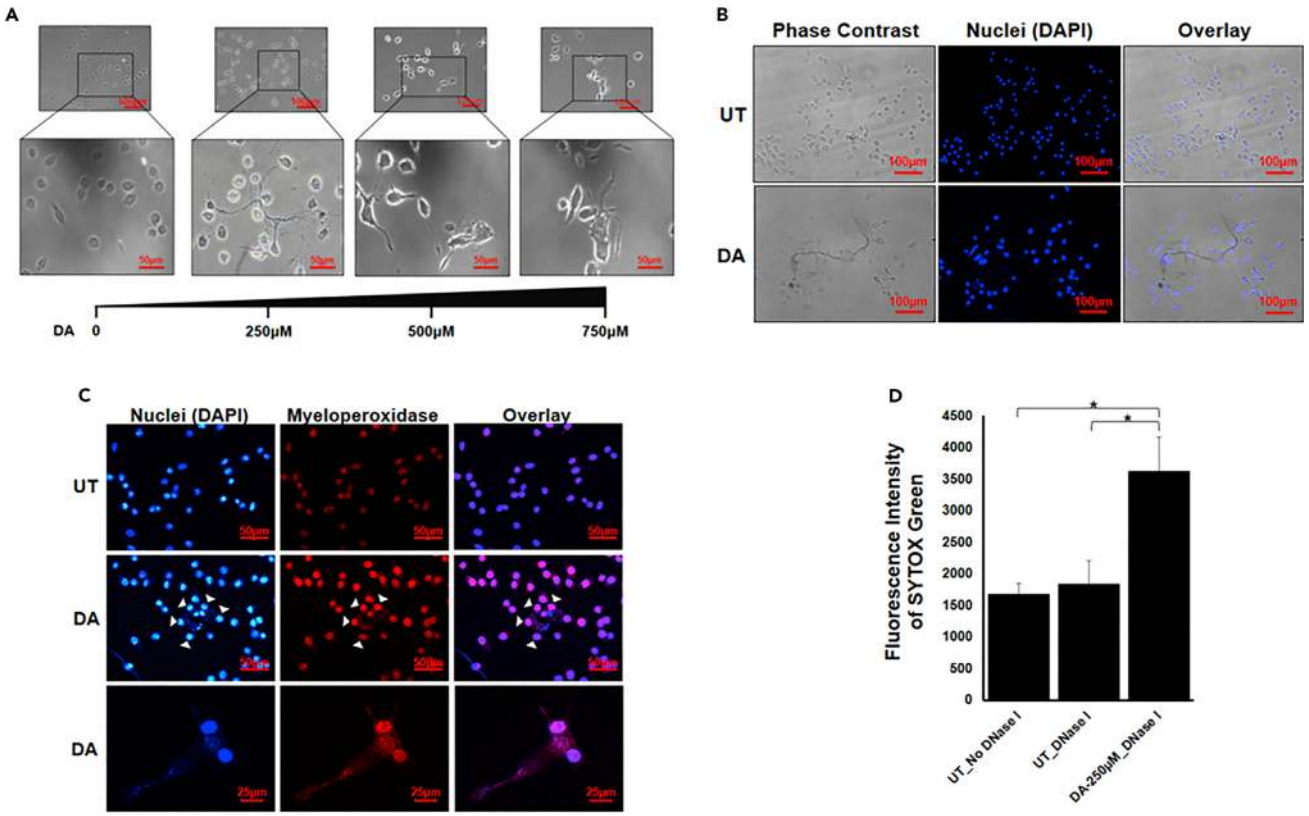

Figure 1. Visualization of DA-induced extracellular traps in BV2 microglia

(A) BV2 microglia were incubated with different concentrations of dopamine (DA) for 24 hr. ETs were clearly visible at all the concentrations of DA. Scale bars, 100μm and 50μm.

(B and C) BV2 microglia were incubated with 250μM of DA for 24 hr. ETs were stained with just DAPI (blue) (B) or DAPI and MPO (C). The images are representative of three experiments. At least 7 frames were imaged per well in a two well chamber slide. Scale bars, 100μm, 50μm, and 25μm.

(D) DNase I was added after 24 hr in DA-treated wells and untreated (UT) wells. Fluorescence was measured in the collected supernatant with the help of SYTOX Green. Graph is representative of 4 experiments. Data are represented as mean ± SEM. *$p < 0.05$ (Student's t-test).

DA-induced ETs as evident from immunofluorescence images (Figure 3B). These results confirmed that DA induces ET formation in BV2 microglia cell via an ROS-independent pathway.

Extracellular trap formation in BV2 microglia cells is independent of actin polymerization

Actin dynamics may play a role in the formation of ETs (Metzler et al., 2014). To investigate whether actin polymerization plays a role in ET formation in microglia, we preincubated BV2 cells with CytoD and then treated them with DA (Figure 4). Immunofluorescence images confirmed that DA induced ET formation independent of actin polymerization, but the viability of cells was significantly reduced—also seen in MTT assays (Figure 2). This indicates that CytoD- and DA-treated BV2 cells may follow lytic ETosis.

Dopamine-induced extracellular traps are functional

We further investigated whether DA-induced BV2 microglia ETs are functional and can trap bacteria. We incubated (fluorescein) FITC-tagged *E. coli* with BV2 cells treated with only DA, NAC + DA (Figures 5A and 5B), or CytoD + DA (Figure S1). Immunofluorescence microscopy images confirmed that DA-induced ETs are functional and capture *E. coli*. NAC had no effect on the functionality of traps; however, CytoD reduced the functionality of traps (Figure S1).

Dopamine induces extracellular traps in primary human microglia

It was clear from our results that DA induces functional ETs in BV2 microglia cell line. We extended our investigation to primary adult human microglia. We isolated primary adult human microglia, as described

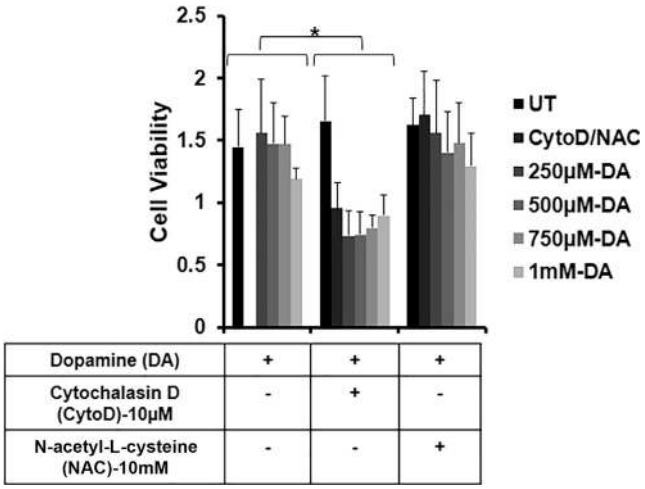

Dopamine (DA)	+	+	+
Cytochalasin D (CytoD)-10μM	-	+	-
N-acetyl-L-cysteine (NAC)-10mM	-	-	+

Figure 2. Dopamine induces extracellular traps formation independent of cell death

BV2 microglia were seeded in a 96-well microplate and were pretreated with 10μM cytochalasin D (CytoD) for 20 min and 10mM N-acetyl-L-cysteine (NAC) for 3 hr. Pretreatment was followed by dopamine (DA) treatment for 24 hr. Cell viability was observed by taking the absorbance at 570 nm. The graph is representative of 3 experiments. Data are represented as mean ± SEM. *p < .05 (Student's t-test).

previously (Agrawal et al., 2020), and characterized them by staining with *Ricinus communis agglutinin* (RCA) (Figures 6A and S2). To determine whether DA can induce ETs in primary human microglia, we treated the isolated cells with 2.5μM DA for 12 hours (Figure 6). We stained the cells with RCA (green), as a microglial marker, as well as DAPI (blue) and anti-DNA/Histone H1 antibody (red) for ETs (Figure 6B). Immunofluorescence images confirmed that DA induces ETs in primary human microglia.

Microglia extracellular traps are present in glioblastoma

Recent studies suggest that GBM cells express DR2 and secrete DA (Caragher et al., 2019; Weissenrieder et al., 2019). These findings encouraged us to investigate whether microglia present in the GBM microenvironment form extracellular traps. We stained GBM tissues with RCA for microglia (green) and H1/DNA antibody for ETs (red). H1/DNA staining was uniformly distributed inside the cells' nucleus in the human cerebrum tissue, whereas it showed a punctate staining around the cells in case of GBM tissues (Figures 7 and S3). Overlap of H1/DNA and RCA confirmed the formation of ETs by microglia. An algorithm was developed to quantify the formation of ETs. GBM tissues showed significant formation of ETs. There are cells other than microglia that are also showing punctate stain. This may be because of the presence of neutrophils and other cells within GBM tissue (Chen and Hambardzumyan, 2018; Schiffer et al., 2018) that are known to form ETs.

DISCUSSION

ETs play a critical role in health and disease (Daniel et al., 2019; Linders and Madhi, 2020; Papayannopoulos, 2017). We establish that DA can induce formation of ETs in BV2 microglia and primary adult human microglia (Figures 1 and 6). Presence of DA receptors on microglia and cells of adaptive and innate immune system points toward DA's role in immune regulation (Pocock and Kettenmann, 2007; Mckenna et al., 2002; Sookhai et al., 1999). The ability of DA to induce ETs points toward the role of DA in immune regulation and sterile inflammation. Lymphocytes and dendritic cells can produce DA that can act in an autocrine and/or paracrine manner (Cosentino et al., 2007; Mckenna et al., 2002; Nakano et al., 2009). DA concentration varies in different regions of the brain and can increase up to 1800μM (Ewing et al., 1983; Olefirowicz and Ewing, 1990; Basu et al., 2001; Yan et al., 2015; Goto et al., 2007; Lucas and McMillen, 2002; Matt and Gaskill, 2020). Our results provide a pivotal link between DA and neuro-inflammation.

Cells forming ETs via the suicidal NETosis pathway die immediately while cells following the vital NETosis pathway survive and continue to function normally (Papayannopoulos, 2017; Yipp and Kubes, 2013). We performed MTT assays to investigate the toxicity of DA on BV2 microglia and established that DA is not

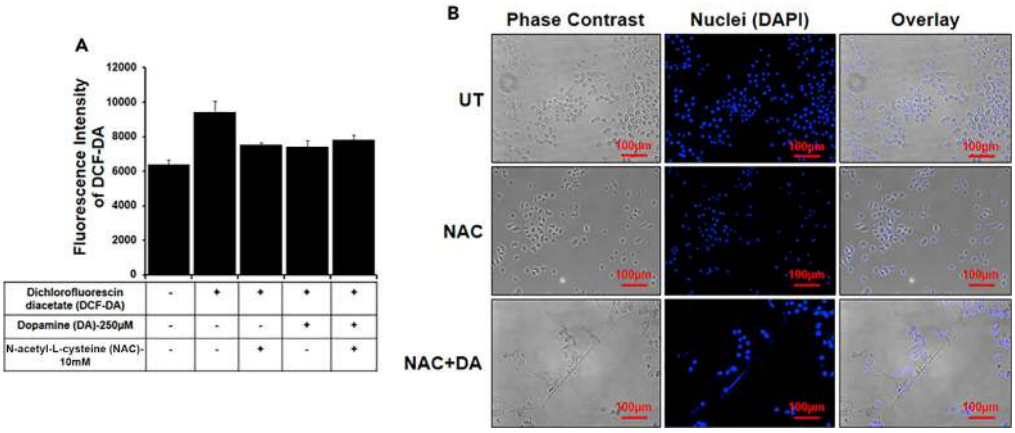

Figure 3. Dopamine induces extracellular traps independent of ROS

Cells were pretreated with 10mM N-acetyl-L-cysteine (NAC) for 3 hr followed by 250μM dopamine (DA) treatment for 24 hr.

(A) ROS production was checked with the help of dichlorofluorescin diacetate (DCF-DA). The graph is representative of three experiments. Data are represented as mean ± SEM.

(B) ET formation was induced by DA even in the presence of NAC. ETs were stained with DAPI (blue). At least 7 frames were imaged per well. Scale bars, 100μm.

cytotoxic (Figure 2). This implies that DA-induced ET formation in BV2 microglia does not lead to immediate cell death. Yousefi et al. first showed that neutrophils can survive even after the formation of NETs. Interestingly, the traps formed by viable neutrophils contained mitochondrial DNA instead of nuclear DNA (Yousefi et al., 2009). How long does microglia survive after expelling its DNA and what is the composition of microglia ETs are intriguing areas for future investigations.

Another aspect of the mechanism we observed was that DA-induced ETs follow an ROS-independent pathway. DA can work as an antioxidant (Jodko-Piórecka and Litwinienko, 2015), and our results showed that DA did not induce significant ROS generation in BV2 microglia (Figure 3). We pretreated cells with the ROS scavenger NAC and then with DA to confirm no significant increase in ROS levels. These results proposed that DA-induced ET formation is independent of ROS. We confirmed this by observing the formation of traps even when ROS was inhibited (Figure 3). ROS-independent ET formation is previously reported to follow vital ETosis (Pilsczek et al., 2010). The molecules involved in this pathway are under-explored. ET formation is highly stimulus dependent (Daniel et al., 2019; Papayannopoulos, 2017; Doster et al., 2017). Our result is crucial, as evidence of different stimuli inducing vital ETosis will help in exploring molecular pathways. Actin dynamics plays a crucial role in

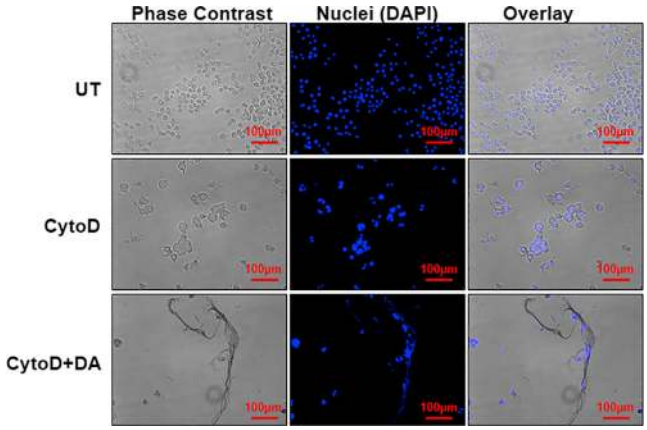

Figure 4. Extracellular trap formation is independent of actin polymerization

Cells were pretreated for 20 min with 10μM cytochalasin D (CytoD) followed by treatment with 250μM dopamine (DA) for 24 hr. Inhibition of actin polymerization had no effect on ET formation. ETs were stained with DAPI (blue). The images are the representative of two experiments. At least 7 frames were imaged per well. Scale bars, 100μm.

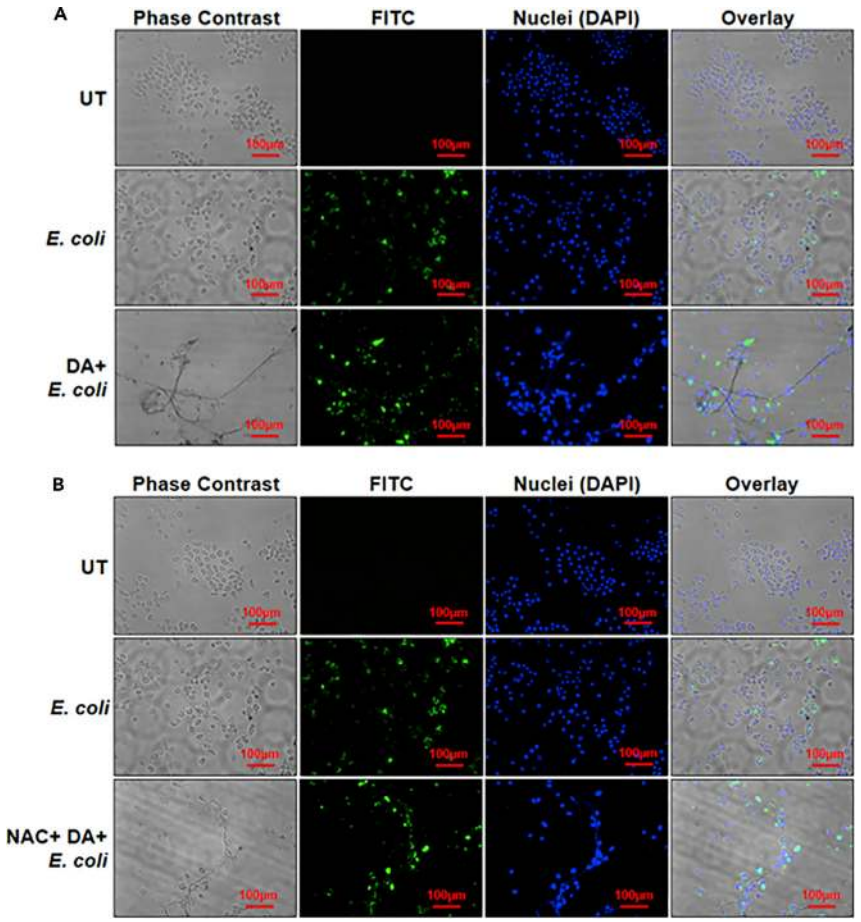

Figure 5. Dopamine induces formation of functional extracellular traps

(A) BV2 microglia were incubated with dopamine (DA) for 3 hr. FITC-tagged *E. coli* (green) was added followed by DA incubation, and cells were further incubated for 21 hours. ETs were stained with DAPI (blue). In the overlay image, green dots are overlapping with the blue ETs, suggesting that ETs are trapping *E. coli*. Images are representative of two experiments. At least 7 frames were imaged per well. Scale bars, 100μm. (B) BV2 microglia were pretreated with N-acetyl-L-cysteine (NAC) and were incubated with dopamine (DA) for 3 hr. FITC-tagged *E. coli* (green) was added followed by DA incubation, and cells were further incubated for 21 hours. ETs were stained with DAPI (blue). In the overlay image, green dots are overlapping with the blue ETs, suggesting that ETs are trapping *E. coli*. Images are representative of two experiments. At least 7 frames were imaged per well. Scale bars, 100μm.

ET formation (Stojkov et al., 2017; Metzler et al., 2014). But sometimes inhibition of actin polymerization does not affect ET formation (Abi Abdallah et al., 2012; Granger et al., 2017). We observed that DA induces ETs in an actin polymerization independent manner in BV2 cells (Figure 4). It was evident that CytoD does not affect ET formation, but it was cytotoxic as evident from our MTT assay. Inhibiting actin polymerization may induce lytic ETosis in BV2 cells. ETs are hypothesized as an alternate mechanism adopted by immune cells to counter pathogens when their phagocytic capacity is overwhelmed (Branzk et al., 2014). It is possible that, in some cases, inhibiting phagocytosis might push immune cells toward ETs inducing pathways. One of the key functions of ETs is to trap pathogens (Brinkmann et al., 2004; Doster et al., 2017; Papayannopoulos, 2017). DA-induced ETs in BV2 cells successfully trapped FITC-tagged *E. coli* (Figure 5). Even the ETs formed in presence of NAC or CytoD (Figure S1) trapped *E. coli*. Thus, inhibition of ROS did not affect functionality of traps. But functionality of traps was compromised in CytoD-treated cells. How CytoD affects ET formation and functionality in microglia needs further investigation. These results established trap formation as an important mechanism of microglial response to counter pathogens.

Encouraged by the results from BV2 microglia, we treated primary human adult microglia with known ET inducers, PMA and LPS (Doster et al., 2017; Papayannopoulos, 2017), and DA; we observed the formation of

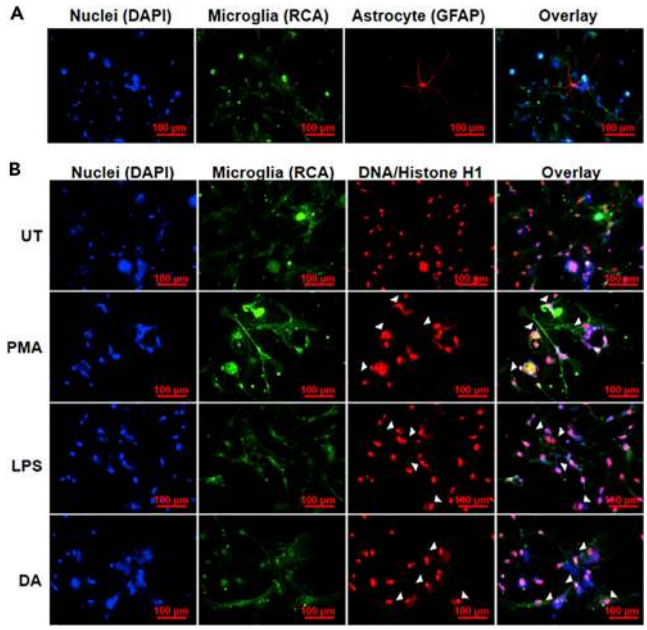

Figure 6. Dopamine induces extracellular traps in primary human microglia

(A) Primary human microglia isolated from adult human brain tissues. RCA (green) was used as a microglia marker, and glial fibrillary acidic protein (GFAP) (red) was used as an astrocyte marker. About 80% of the cells isolated were microglia. (B) Isolated microglia were treated with 2.5μM dopamine (DA) for 12 hr. RCA (green) was used as a microglia marker. ETs (arrow heads) were visualized using DAPI (blue) and DNA/Histone H1 antibodies (red). At least 7 frames were imaged per well of the two well chamber slide. Scale bars, 100μm.

ETs (Figure 6B). This was exciting and it opened new avenues of microglia ET exploration. PMA and LPS induce ETs in different cells primarily via an ROS-dependent lytic pathway (Fuchs et al., 2007; Khan et al., 2017) while our results in BV2 cells suggest an ROS-independent non-lytic pathway for microglia ET formation. Our results support the heterogeneity of ET formation pathway adopted by cells depending on the stimuli (Petretto et al., 2019; Pieterse et al., 2016; Daniel et al., 2019). ETs are protective and inflammatory (Daniel et al., 2019). They play role in pathogenesis of many diseases including cancer (Daniel et al., 2019; Papayannopoulos, 2017). A recent report by Caragher et al. shows that GBM cells express DR2 and they can synthesize and secrete DA (Caragher et al., 2019). This may increase local concentration of DA within the tumor microenvironment which is yet to be quantified. We found that microglia present in the GBM microenvironment form ETs (Figure 7). Inflammation caused by ETs might be involved in progression of GBM. ETs play a role in metastasis of cancer, and cancer cells in turn can induce ETs (Cools-Lartigue et al., 2013; Tohme et al., 2016; Park et al., 2016). It is necessary to explore if that is true for GBM. Several key questions need future investigations; what is the role of microglia ETs in GBM pathology? Are ETs involved in shaping the microenvironment of GBM or inflammation? Microglia ETs present in the GBM need thorough characterization. It will help us in better elucidating their role in GBM and its microenvironment. ETs play an important role in autoimmune diseases such as lupus and arthritis (Garcia-Romo et al., 2011; Khandpur et al., 2013; Yu and Su, 2013). Our findings that DA can induce ETs point toward a role of DA in other inflammatory diseases in the brain. In diseases like schizophrenia, Tourette syndrome, Parkinson disease, and multiple sclerosis, DA plays a substantial role in the pathophysiology (Arreola et al., 2016; Denys et al., 2013; Brisch et al., 2014). Studying DA-induced microglial ETs may lead to interventions that may help in better management of these disease and GBM.

Limitations of the study

In the present study, we have shown formation of DA-induced microglia extracellular traps composed of DNA. Mitochondrial DNA or/and nuclear DNA contributes to formation of ETs (Lood et al., 2016; Mcilroy et al., 2014). This study does not show whether traps are composed of nuclear DNA or/and mitochondrial DNA. Studying this will help in further elucidating the intermediate signaling molecules involved in extracellular trap formation. We have shown that the traps are functional as they are capable of trapping FITC-tagged *E. coli*. But the functionality of traps also depends on traps killing bacteria. We have not evaluated

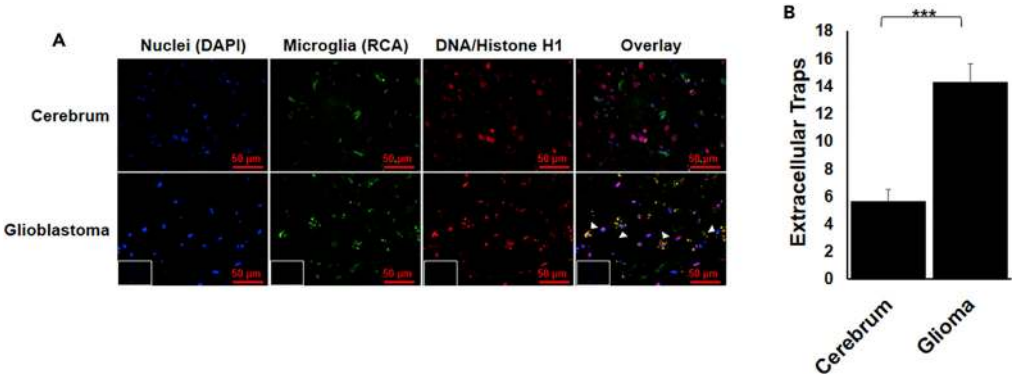

Figure 7. Presence of microglia extracellular traps in GBM

(A) GBM tissue was stained with DAPI (blue), RCA (green) for microglia, and DNA/Histone H1 (red) for ETs. The formation of ETs by microglia can be visualized by the punctate red staining overlapping with green (arrow heads). Inset represents secondary antibody control. Scale bars, 50μm.

(B) The punctate red staining overlapping with green was quantified. The graph represents average of the quantified value. The result is representative of two experiments. At least 7 frames were imaged per section and quantified. Data are represented as mean ± SEM. ***$p < .0001$ (Student's t-test).

whether the traps are capable of killing bacteria which will establish effective functionality of the traps. Protein composition of the traps also varies with cells and stimuli (Papayannopoulos, 2017). As ETs can be inflammatory, extension of this study is needed to characterize microglia ETs to determine their nature.

Resource availability

Lead contact

Further information and requests for resources should be directed to and will be fulfilled by the Lead Contact, Dr. Sushmita Jha (sushmitajha@iitj.ac.in).

Material availability

All unique/stable reagents generated in this study are available from the Lead Contact with a completed Materials Transfer Agreement.

Data and code availability

The published article includes all code generated during this study. Original data have been deposited to Mendley Data: https://doi.org/10.17632/k2r3xsyh2m.1.

METHODS

All methods can be found in the accompanying Transparent Methods supplemental file.

SUPPLEMENTAL INFORMATION

Supplemental Information can be found online at https://doi.org/10.1016/j.isci.2020.101968.

ACKNOWLEDGMENTS

S.J.'s laboratory was established with institutional grants from Indian Institute of Technology Jodhpur (IITJ) and is funded by grants from the Department of Biotechnology (BT/PR12831/MED/30/1489/2015) and the Ministry of Electronics and Information Technology, Government of India (No.4 (16)/2019-ITEA). We thank Dr. Anirban Basu's Lab at National Brain Research Center (NBRC), India, for their kind gift of the BV2 microglia cell line. Modified histone antibodies were a kind gift from Dr. Vijayalakshmi Mahadevan from the Institute of Bioinformatics and Applied Biotechnology. Human brain tissue sections were obtained from the All India Institute of Medical Sciences (AIIMS) Jodhpur and Tata Memorial Hospital, Tata Memorial Center, Mumbai, Maharashtra, India. We thank Dr. Pushpa Potaliya and Dr. Vineet Jain, Department of Anatomy, AIIMS, Jodhpur, for valuable assistance in histological processing of the tissues. We thank Mr. Bharat Pareek, Technical Superintendent, Indian Institute of Technology Jodhpur, for his technical support in our lab.

AUTHOR CONTRIBUTIONS

I.A. designed and performed the experiments (data analysis, standardized primary microglia isolation, immunofluorescence), as well as prepared and edited initial manuscript draft. N.S. performed BV2 microglia cell culture. S.S. did some immunocytochemistry experiments. D.B.C. wrote the code for ET quantification and D.C. and S.A. helped with quantification. D.J. provided brain tissues for microglia isolation. S.G., S.E., and T.G. provided tissue sections for IHC studies. S.J. conceptualized the study, designed experiments, wrote initial draft, and edited and reviewed the manuscript. All authors reviewed the manuscript.

DECLARATION OF INTERESTS

The authors declare no competing interests.

Received: September 11, 2020
Revised: November 26, 2020
Accepted: December 16, 2020
Published: January 22, 2021

REFERENCES

Abi Abdallah, D.S., Lin, C., Ball, C.J., King, M.R., Duhamel, G.E., and Denkers, E.Y. (2012). Toxoplasma gondii triggers release of human and mouse neutrophil extracellular traps. Infect. Immun. *80*, 768–777.

Agrawal, I., Saxena, S., Nair, P., Jha, D., and Jha, S. (2020). Obtaining Human Microglia from Adult Human Brain Tissue. JoVE *162*, e61438.

Arreola, R., Alvarez-Herrera, S., Pérez-Sánchez, G., Becerril-Villanueva, E., Cruz-Fuentes, C., Flores-Gutierrez, E.O., Garcés-Alvarez, M.E., De La Cruz-Aguilera, D.L., Medina-Rivero, E., Hurtado-Alvarado, G., et al. (2016). Immunomodulatory effects mediated by dopamine. J. Immunol. Res. *2016*, 3160486.

Basu, S., Nagy, J.A., Pal, S., Vasile, E., Eckelhoefer, I.A., Susan Bliss, V., Manseau, E.J., Dasgupta, P.S., Dvorak, H.F., and Mukhopadhyay, D. (2001). The neurotransmitter dopamine inhibits angiogenesis induced by vascular permeability factor/vascular endothelial growth factor. Nat. Med. *7*, 569–574.

Beninger, R.J. (1983). The role of dopamine in locomotor activity and learning. Brain Res. *287*, 173–196.

Branzk, N., Lubojemska, A., Hardison, S.E., Wang, Q., Gutierrez, M.G., Brown, G.D., and Papayannopoulos, V. (2014). Neutrophils sense microbe size and selectively release neutrophil extracellular traps in response to large pathogens. Nat. Immunol. *15*, 1017.

Brinkmann, V., Reichard, U., Goosmann, C., Fauler, B., Uhlemann, Y., Weiss, D.S., Weinrauch, Y., and Zychlinsky, A. (2004). Neutrophil extracellular traps kill bacteria. Science *303*, 1532.

Brisch, R., Saniotis, A., Wolf, R., Bielau, H., Bernstein, H.-G., Steiner, J., Bogerts, B., Braun, K., Jankowski, Z., Kumaratilake, J., et al. (2014). The role of dopamine in schizophrenia from a neurobiological and evolutionary perspective: old fashioned, but still in vogue. Front. Psychiatry *5*, 47.

Bryukhin, G.V., and Shopova, A.V. (2015). Characteristics of mononuclear extracellular traps in the offspring of female rats with drug-induced hepatitis. Bull. Exp. Biol. Med. *159*, 435–437.

Caragher, S.P., Shireman, J.M., Huang, M., Miska, J., Atashi, F., Baisiwala, S., Hong Park, C., Saathoff, M.R., Warnke, L., Xiao, T., et al. (2019). Activation of dopamine receptor 2 prompts transcriptomic and metabolic plasticity in glioblastoma. J. Neurosci. *39*, 1982.

Caudrillier, A., Kessenbrock, K., Gilliss, B.M., Nguyen, J.X., Marques, M.B., Monestier, M., Toy, P., Werb, Z., and Looney, M.R. (2012). Platelets induce neutrophil extracellular traps in transfusion-related acute lung injury. J. Clin. Invest. *122*, 2661–2671.

Cedervall, J., Zhang, Y., Huang, H., Zhang, L., Femel, J., Dimberg, A., and Olsson, A.-K. (2015). Neutrophil extracellular traps accumulate in peripheral blood vessels and compromise organ function in tumor-bearing animals. Cancer Res. *75*, 2653.

Chen, Z., and Hambardzumyan, D. (2018). Immune microenvironment in glioblastoma subtypes. Front. Immunol. *9*, 1004.

Chow, O.A., Von Köckritz-Blickwede, M., Bright, A.T., Hensler, M.E., Zinkernagel, A.S., Cogen, A.L., Gallo, R.L., Monestier, M., Wang, Y., Glass, C.K., and Nizet, V. (2010). Statins enhance formation of phagocyte extracellular traps. Cell Host Microbe *8*, 445–454.

Cools-Lartigue, J., Spicer, J., Mcdonald, B., Gowing, S., Chow, S., Giannias, B., Bourdeau, F., Kubes, P., and Ferri, L. (2013). Neutrophil extracellular traps sequester circulating tumor cells and promote metastasis. J. Clin. Invest. *123*, 3446–3458.

Cosentino, M., Fietta, A.M., Ferrari, M., Rasini, E., Bombelli, R., Carcano, E., Saporiti, F., Meloni, F., Marino, F., and Lecchini, S. (2007). Human CD4+CD25+ regulatory T cells selectively express tyrosine hydroxylase and contain endogenous catecholamines subserving an autocrine/paracrine inhibitory functional loop. Blood *109*, 632–642.

Czaikoski, P.G., Mota, J.M.S.C., Nascimento, D.C., Sônego, F., Castanheira, F.V.E.S., Melo, P.H., Scortegagna, G.T., Silva, R.L., Barroso-Sousa, R., Souto, F.O., et al. (2016). Neutrophil extracellular traps induce organ damage during experimental and clinical sepsis. PLoS One *11*, e0148142.

Daniel, C., Leppkes, M., Muñoz, L.E., Schley, G., Schett, G., and Herrmann, M. (2019). Extracellular DNA traps in inflammation, injury and healing. Nat. Rev. Nephrol. *15*, 559–575.

Delgado-Rizo, V., Martínez-Guzmán, M., Iñiguez-Gutierrez, L., García-Orozco, A., Alvarado-Navarro, A., and Fafutis-Morris, M. (2017). Neutrophil extracellular traps and its implications in inflammation: an overview. Front. Immunol. *8*, 81.

Demers, M., Krause, D.S., Schatzberg, D., Martinod, K., Voorhees, J.R., Fuchs, T.A., Scadden, D.T., and Wagner, D.D. (2012). Cancers predispose neutrophils to release extracellular DNA traps that contribute to cancer-associated thrombosis. Proc. Natl. Acad. Sci. U S A *109*, 13076–13081.

Denys, D., De Vries, F., Cath, D., Figee, M., Vulink, N., Veltman, D.J., Van Der Doef, T.F., Boellaard, R., Westenberg, H., Van Balkom, A., et al. (2013). Dopaminergic activity in Tourette syndrome and obsessive-compulsive disorder. Eur. Neuropsychopharmacol. *23*, 1423–1431.

Doster, R.S., Rogers, L.M., Gaddy, J.A., and Aronoff, D.M. (2017). Macrophage extracellular traps: a scoping review. J. Innate Immun. *10*, 3–13.

Dwyer, M., Shan, Q., D'ortona, S., Maurer, R., Mitchell, R., Olesen, H., Thiel, S., Huebner, J., and Gadjeva, M. (2014). Cystic Fibrosis Sputum DNA has NETosis characteristics and NET release is regulated by MIF. J. Innate Immun. *6*, 765–779.

Ewing, A.G., Bigelow, J.C., and Wightman, R.M. (1983). Direct in vivo monitoring of dopamine released from two striatal compartments in the rat. Science *221*, 169.

Fan, Y., Chen, Z., Pathak, J.L., Carneiro, A.M.D., and Chung, C.Y. (2018). Differential regulation of adhesion and phagocytosis of resting and

activated microglia by dopamine. Front. Cell. Neurosci. *12*, 309.

Ferreri, L., Mas-Herrero, E., Zatorre, R.J., Ripollés, P., Gomez-Andres, A., Alicart, H., Olivé, G., Marco-Pallarés, J., Antonijoan, R.M., Valle, M., et al. (2019). Dopamine modulates the reward experiences elicited by music. Proc. Natl. Acad. Sci. U S A *116*, 3793.

Fuchs, T.A., Abed, U., Goosmann, C., Hurwitz, R., Schulze, I., Wahn, V., Weinrauch, Y., Brinkmann, V., and Zychlinsky, A. (2007). Novel cell death program leads to neutrophil extracellular traps. J. Cell. Biol. *176*, 231–241.

Fuchs, T.A., Brill, A., Duerschmied, D., Schatzberg, D., Monestier, M., Myers, D.D., Wrobleski, S.K., Wakefield, T.W., Hartwig, J.H., and Wagner, D.D. (2010). Extracellular DNA traps promote thrombosis. Proc. Natl. Acad. Sci. U S A *107*, 15880–15885.

Garcia-Romo, G.S., Caielli, S., Vega, B., Connolly, J., Allantaz, F., Xu, Z., Punaro, M., Baisch, J., Guiducci, C., Coffman, R.L., et al. (2011). Netting neutrophils are major inducers of type I IFN production in pediatric systemic lupus erythematosus. Sci. Transl. Med. *3*, 73ra20.

Goto, Y., Otani, S., and Grace, A.A. (2007). The Yin and Yang of dopamine release: a new perspective. Neuropharmacology *53*, 583–587.

Granger, V., Faille, D., Marani, V., Noël, B., Gallais, Y., Szely, N., Flament, H., Pallardy, M., Chollet-Martin, S., and De Chaisemartin, L. (2017). Human blood monocytes are able to form extracellular traps. J. Leukoc. Biol. *102*, 775–781.

Guglietta, S., Chiavelli, A., Zagato, E., Krieg, C., Gandini, S., Ravenda, P.S., Bazolli, B., Lu, B., Penna, G., and Rescigno, M. (2016). Coagulation induced by C3aR-dependent NETosis drives protumorigenic neutrophils during small intestinal tumorigenesis. Nat. Commun. *7*, 11037.

Gupta, A.K., Joshi, M.B., Philippova, M., Erne, P., Hasler, P., Hahn, S., and Resink, T.J. (2010). Activated endothelial cells induce neutrophil extracellular traps and are susceptible to NETosis-mediated cell death. FEBS Lett. *584*, 3193–3197.

Hakkim, A., Fürnrohr, B.G., Amann, K., Laube, B., Abed, U.A., Brinkmann, V., Herrmann, M., Voll, R.E., and Zychlinsky, A. (2010). Impairment of neutrophil extracellular trap degradation is associated with lupus nephritis. Proc. Natl. Acad. Sci. U S A *107*, 9813–9818.

Halder, L.D., Abdelfatah, M.A., Jo, E.A.H., Jacobsen, I.D., Westermann, M., Beyersdorf, N., Lorkowski, S., Zipfel, P.F., and Skerka, C. (2016). Factor H binds to extracellular DNA traps released from human blood monocytes in response to Candida albicans. Front. Immunol. *7*, 671.

Jodko-Piórecka, K., and Litwinienko, G. (2015). Antioxidant activity of dopamine and L-DOPA in lipid micelles and their cooperation with an analogue of α-tocopherol. Free Radic. Biol. Med. *83*, 1–11.

Jönsson, B.E., Bylund, J., Johansson, B.R., Telemo, E., and Wold, A.E. (2013). Cord-forming mycobacteria induce DNA meshwork formation by human peripheral blood mononuclear cells. Pathog. Dis. *67*, 54–66.

Joshi, M.B., Lad, A., Bharath Prasad, A.S., Balakrishnan, A., Ramachandra, L., and Satyamoorthy, K. (2013). High glucose modulates IL-6 mediated immune homeostasis through impeding neutrophil extracellular trap formation. FEBS Lett. *587*, 2241–2246.

Khan, M.A., Farahvash, A., Douda, D.N., Licht, J.-C., Grasemann, H., Sweezey, N., and Palaniyar, N. (2017). JNK activation turns on LPS- and gram-negative bacteria-induced NADPH oxidase-dependent suicidal NETosis. Sci. Rep. *7*, 3409.

Khandpur, R., Carmona-Rivera, C., Vivekanandan-Giri, A., Gizinski, A., Yalavarthi, S., Knight, J.S., Friday, S., Li, S., Patel, R.M., Subramanian, V., et al. (2013). Nets are a source of citrullinated autoantigens and stimulate inflammatory responses in rheumatoid arthritis. Sci. Transl. Med. *5*, 178ra40.

King, P.T., Sharma, R., O'sullivan, K., Selemidis, S., Lim, S., Radhakrishna, N., Lo, C., Prasad, J., Callaghan, J., Mclaughlin, P., et al. (2015). Nontypeable Haemophilus influenzae induces sustained lung oxidative stress and protease expression. PLoS One *10*, e0120371.

Kolaczkowska, E., Jenne, C.N., Surewaard, B.G.J., Thanabalasuriar, A., Lee, W.-Y., Sanz, M.-J., Mowen, K., Opdenakker, G., and Kubes, P. (2015). Molecular mechanisms of NET formation and degradation revealed by intravital imaging in the liver vasculature. Nat. Commun. *6*, 6673.

Li, Q., and Barres, B.A. (2018). Microglia and macrophages in brain homeostasis and disease. Nat. Rev. Immunol. *18*, 225–242.

Linders, J., and Madhi, R. (2020). Extracellular Cold-Inducible RNA-Binding Protein Regulates Neutrophil Extracellular Trap Formation and Tissue Damage in Acute Pancreatitis (Laboratory Investigation (Nature publishing group)).

Lood, C., Blanco, L.P., Purmalek, M.M., Carmona-Rivera, C., De Ravin, S.S., Smith, C.K., Malech, H.L., Ledbetter, J.A., Elkon, K.B., and Kaplan, M.J. (2016). Neutrophil extracellular traps enriched in oxidized mitochondrial DNA are interferogenic and contribute to lupus-like disease. Nat. Med. *22*, 146.

Lucas, L.A.C., and Mcmillen, B.A. (2002). Differences in brain area concentrations of dopamine and serotonin in myers' high ethanol preferring (mHEP) and outbred rats. J. Neural Transm. *109*, 279–292.

Martinod, K., Demers, M., Fuchs, T.A., Wong, S.L., Brill, A., Gallant, M., Hu, J., Wang, Y., and Wagner, D.D. (2013). Neutrophil histone modification by peptidylarginine deiminase 4 is critical for deep vein thrombosis in mice. Proc. Natl. Acad. Sci. U S A *110*, 8674–8679.

Matt, S.M., and Gaskill, P.J. (2020). Where is dopamine and how do immune cells see it?: dopamine-mediated immune cell function in health and disease. J. Neuroimmune Pharmacol. *15*, 114–164.

Mcilroy, D.J., Jarnicki, A.G., Au, G.G., Lott, N., Smith, D.W., Hansbro, P.M., and Balogh, Z.J. (2014). Mitochondrial DNA neutrophil extracellular traps are formed after trauma and subsequent surgery. J. Crit. Care *29*, 1133.e1–1133.e5.

Mckenna, F., Mclaughlin, P.J., Lewis, B.J., Sibbring, G.C., Cummerson, J.A., Bowen-Jones, D., and Moots, R.J. (2002). Dopamine receptor expression on human T- and B-lymphocytes, monocytes, neutrophils, eosinophils and NK cells: a flow cytometric study. J. Neuroimmunol. *132*, 34–40.

Metzler, Kathleen D., Goosmann, C., Lubojemska, A., Zychlinsky, A., and Papayannopoulos, V. (2014). A myeloperoxidase-containing complex regulates neutrophil elastase release and actin dynamics during NETosis. Cell Rep. *8*, 883–896.

Möllerherm, H., Von Köckritz-Blickwede, M., and Branitzki-Heinemann, K. (2016). Antimicrobial activity of mast cells: role and relevance of extracellular DNA traps. Front. Immunol. *7*, 265.

Morshed, M., Hlushchuk, R., Simon, D., Walls, A.F., Obata-Ninomiya, K., Karasuyama, H., Djonov, V., Eggel, A., Kaufmann, T., Simon, H.-U., and Yousefi, S. (2014). NADPH oxidase–independent formation of extracellular DNA traps by basophils. J. Immunol. *192*, 5314.

Nakano, K., Higashi, T., Takagi, R., Hashimoto, K., Tanaka, Y., and Matsushita, S. (2009). Dopamine released by dendritic cells polarizes Th2 differentiation. Int. Immunol. *21*, 645–654.

Olefirowicz, T.M., and Ewing, A.G. (1990). Dopamine concentration in the cytoplasmic compartment of single neurons determined by capillary electrophoresis. J. Neurosci. Methods *34*, 11–15.

Ott, T., and Nieder, A. (2019). Dopamine and cognitive control in prefrontal cortex. Trends Cogn. Sci. *23*, 213–234.

Papayannopoulos, V. (2017). Neutrophil extracellular traps in immunity and disease. Nat. Rev. Immunol. *18*, 134–147.

Park, J., Wysocki, R.W., Amoozgar, Z., Maiorino, L., Fein, M.R., Jorns, J., Schott, A.F., Kinugasa-Katayama, Y., Lee, Y., Won, N.H., et al. (2016). Cancer cells induce metastasis-supporting neutrophil extracellular DNA traps. Sci. translational Med. *8*, 361ra138.

Peng, H.-H., Liu, Y.-J., Ojcius, D.M., Lee, C.-M., Chen, R.-H., Huang, P.-R., Martel, J., and Young, J.D. (2017). Mineral particles stimulate innate immunity through neutrophil extracellular traps containing HMGB1. Scientific Rep. *7*, 16628.

Petretto, A., Bruschi, M., Pratesi, F., Croia, C., Candiano, G., Ghiggeri, G., and Migliorini, P. (2019). Neutrophil extracellular traps (NET) induced by different stimuli: a comparative proteomic analysis. PLoS One *14*, e0218946.

Pieterse, E., Rother, N., Yanginlar, C., Hilbrands, L.B., and Van Der Vlag, J. (2016). Neutrophils discriminate between lipopolysaccharides of different bacterial sources and selectively release neutrophil extracellular traps. Front. Immunol. *7*, 484.

Pilsczek, F.H., Salina, D., Poon, K.K.H., Fahey, C., Yipp, B.G., Sibley, C.D., Robbins, S.M., Green, F.H.Y., Surette, M.G., Sugai, M., et al. (2010). A novel mechanism of rapid nuclear neutrophil

extracellular trap formation in response to Staphylococcus aureus. J. Immunol. *185*, 7413.

Pocock, J.M., and Kettenmann, H. (2007). Neurotransmitter receptors on microglia. Trends Neurosci. *30*, 527–535.

Saffarzadeh, M., Juenemann, C., Queisser, M.A., Lochnit, G., Barreto, G., Galuska, S.P., Lohmeyer, J., and Preissner, K.T. (2012). Neutrophil extracellular traps directly induce epithelial and endothelial cell death: a predominant role of histones. PLoS One *7*, e32366.

Saitoh, T., Komano, J., Saitoh, Y., Misawa, T., Takahama, M., Kozaki, T., Uehata, T., Iwasaki, H., Omori, H., Yamaoka, S., et al. (2012). Neutrophil extracellular traps mediate a host defense response to human immunodeficiency virus-1. Cell Host Microbe *12*, 109–116.

Schiffer, D., Annovazzi, L., Casalone, C., Corona, C., and Mellai, M. (2018). Glioblastoma: microenvironment and niche concept. Cancers *11*, 5.

Schorn, C., Janko, C., Latzko, M., Chaurio, R., Schett, G., and Herrmann, M. (2012). Monosodium urate crystals induce extracellular DNA traps in neutrophils, eosinophils, and basophils but not in mononuclear cells. Front. Immunol. *3*, 277.

Shen, F., Tang, X., Cheng, W., Wang, Y., Wang, C., Shi, X., An, Y., Zhang, Q., Liu, M., Liu, B., and Yu, L. (2016). Fosfomycin enhances phagocyte-mediated killing of Staphylococcus aureus by extracellular traps and reactive oxygen species. Sci. Rep. *6*, 19262.

Sookhai, S., Wang, J.H., Mccourt, M., O'connell, D., and Redmond, H.P. (1999). Dopamine induces neutrophil apoptosis through a dopamine D-1 receptor-independent mechanism. Surgery *126*, 314–322.

Stojkov, D., Amini, P., Oberson, K., Sokollik, C., Duppenthaler, A., Simon, H.-U., and Yousefi, S. (2017). ROS and glutathionylation balance cytoskeletal dynamics in neutrophil extracellular trap formation. J. Cell Biol. *216*, 4073.

Tohme, S., Yazdani, H.O., Al-Khafaji, A.B., Chidi, A.P., Loughran, P., Mowen, K., Wang, Y., Simmons, R.L., Huang, H., and Tsung, A. (2016). Neutrophil extracellular traps promote the development and progression of liver metastases after surgical stress. Cancer Res. *76*, 1367–1380.

Urban, C.F., Reichard, U., Brinkmann, V., and Zychlinsky, A. (2006). Neutrophil extracellular traps capture and kill Candida albicans yeast and hyphal forms. Cell Microbiol. *8*, 668–676.

Villanueva, E., Yalavarthi, S., Berthier, C.C., Hodgin, J.B., Khandpur, R., Lin, A.M., Rubin, C.J., Zhao, W., Olsen, S.H., Klinker, M., et al. (2011). Netting neutrophils induce endothelial damage, infiltrate tissues and expose immunostimulatory molecules in systemic lupus erythematosus. J. Immunol. *187*, 538–552.

Wang, C., Wang, Y., Shi, X., Tang, X., Cheng, W., Wang, X., An, Y., Li, S., Xu, H., Li, Y., et al. (2019). The TRAPs from microglial vesicles protect against Listeria infection in the CNS. Front. Cell. Neurosci. *13*, 199.

Warnatsch, A., Ioannou, M., Wang, Q., and Papayannopoulos, V. (2015). Neutrophil extracellular traps license macrophages for cytokine production in atherosclerosis. Science *349*, 316.

Webster, S.J., Daigneault, M., Bewley, M.A., Preston, J.A., Marriott, H.M., Walmsley, S.R., Read, R.C., Whyte, M.K.B., and Dockrell, D.H. (2010). Distinct cell death programs in monocytes regulate innate responses following challenge with common causes of invasive bacterial disease. J. Immunol. *185*, 2968–2979.

Weissenrieder, J.S., Reed, J.L., Green, M.V., Moldovan, G.L., Koubek, E.J., Neighbors, J.D., and Hohl, R.J. (2019). The dopamine D2 receptor contributes to the spheroid formation behavior of U87 glioblastoma cells. Pharmacology *105*, 19–27.

Wong, K.-W., and Jacobs, W.R. (2013). Mycobacterium tuberculosis exploits human interferon γ to stimulate macrophage extracellular trap formation and necrosis. J. Infect. Dis. *208*, 109–119.

Wright, T.K., Gibson, P.G., Simpson, J.L., Mcdonald, V.M., Wood, L.G., and Baines, K.J. (2016). Neutrophil extracellular traps are associated with inflammation in chronic airway disease. Respirology *21*, 467–475.

Yan, Y., Jiang, W., Liu, L., Wang, X., Ding, C., Tian, Z., and Zhou, R. (2015). Dopamine controls systemic inflammation through inhibition of NLRP3 inflammasome. Cell *160*, 62–73.

Yipp, B.G., and Kubes, P. (2013). NETosis: how vital is it? Blood *122*, 2784–2794.

Yipp, B.G., Petri, B., Salina, D., Jenne, C.N., Scott, B.N.V., Zbytnuik, L.D., Pittman, K., Asaduzzaman, M., Wu, K., Meijndert, H.C., et al. (2012). Infection-induced NETosis is a dynamic process involving neutrophil multitasking in vivo. Nat. Med. *18*, 1386.

Yoshioka, Y., Sugino, Y., Tozawa, A., Yamamuro, A., Kasai, A., Ishimaru, Y., and Maeda, S. (2016). Dopamine inhibits lipopolysaccharide-induced nitric oxide production through the formation of dopamine quinone in murine microglia BV-2 cells. J. Pharmacol. Sci. *130*, 51–59.

Yousefi, S., Gold, J.A., Andina, N., Lee, J.J., Kelly, A.M., Kozlowski, E., Schmid, I., Straumann, A., Reichenbach, J., Gleich, G.J., and Simon, H.-U. (2008). Catapult-like release of mitochondrial DNA by eosinophils contributes to antibacterial defense. Nat. Med. *14*, 949.

Yousefi, S., Mihalache, C., Kozlowski, E., Schmid, I., and Simon, H.U. (2009). Viable neutrophils release mitochondrial DNA to form neutrophil extracellular traps. Cell Death Differ. *16*, 1438–1444.

Yousefi, S., Stojkov, D., Germic, N., Simon, D., Wang, X., Benarafa, C., and Simon, H.-U. (2019). Untangling "NETosis" from NETs. Eur. J. Immunol. *49*, 221–227.

Yu, Y., and Su, K. (2013). Neutrophil extracellular traps and systemic lupus erythematosus. J. Clin. Cell. Immunol. *4*, 139.

iScience, Volume *24*

Supplemental Information

Dopamine induces functional extracellular traps in microglia

Ishan Agrawal, Nidhi Sharma, Shivanjali Saxena, S. Arvind, Debayani Chakraborty, Debarati Bhunia Chakraborty, Deepak Jha, Surajit Ghatak, Sridhar Epari, Tejpal Gupta, and Sushmita Jha

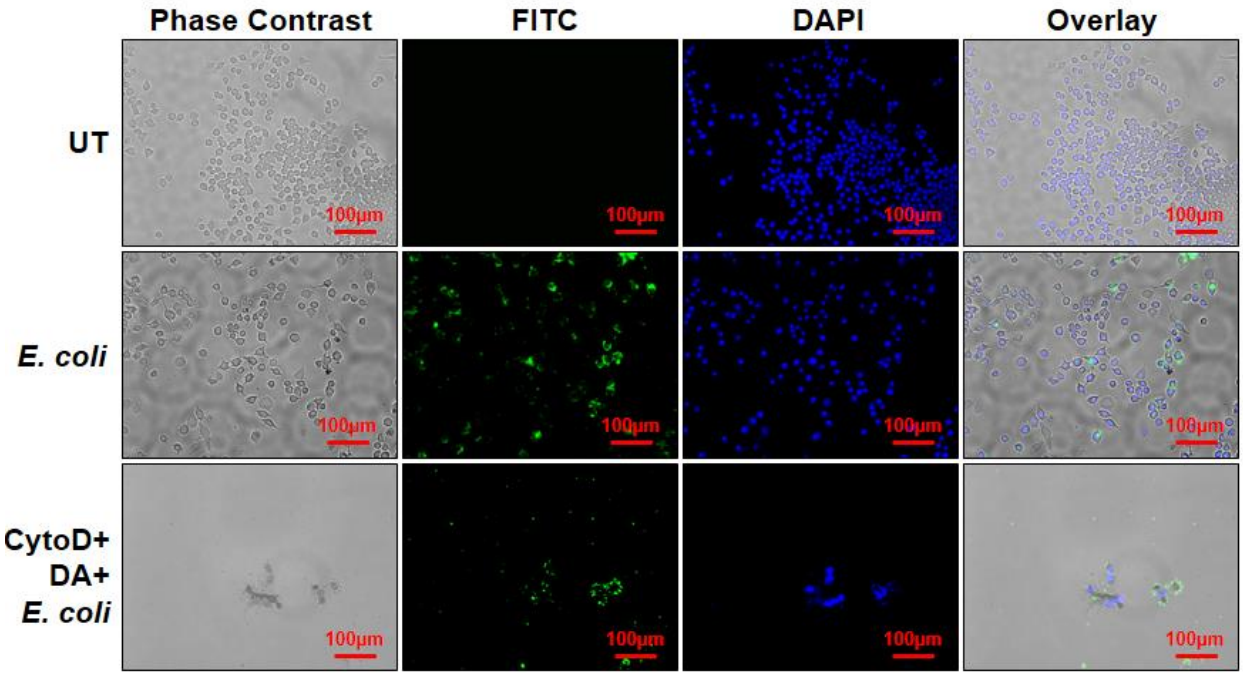

Figure S1. Dopamine Induces Formation of Functional Extracellular Traps Independent of Actin Polymerization, Related to Figure 5. BV2 microglia were pretreated with Cytochalasin D (CytoD) and were incubated with DA for 3 hours. FITC tagged *E. coli* (green) was added followed by DA incubation and cells were further incubated for 21 hours. ETs were stained with DAPI (blue). In the merged image green dots are overlapping with the blue ET suggesting that ETs are trapping *E. coli*. The images are the representative of two experiments. At least 7 frames were imaged per well of the two well chamber slide. Scale bars, 100µm.

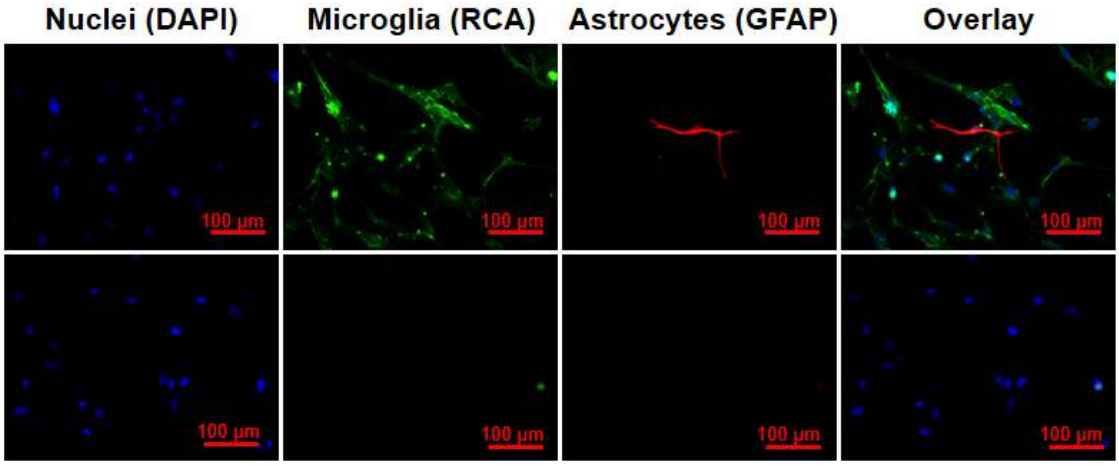

Figure S2. Primary Microglia Isolation from Adult Human Brain Tissue, Related to Figure 6. Primary human microglial isolated from adult human brain tissues. RCA (Green) was used as microglia marker and GFAP (Red) was used as astrocyte marker. About 80% of the cells isolated were microglia. Scale bars, 100µm.

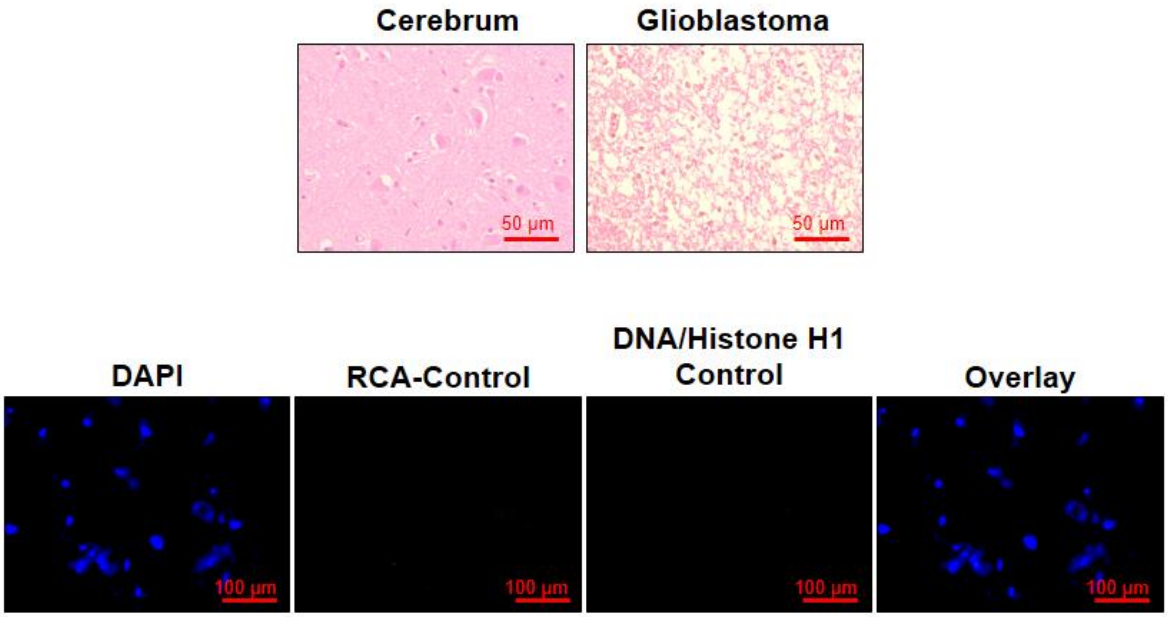

Figure S3. H & E Image, RCA Control and Secondary Antibody Control for DNA/Histone H1, Related to Figure 7. Scale bars, 50µm and 100µm.

Table S1. Patient information for the tissues used for IHC. Related to Figure 7.

Serial no.	Dianosis	Age/Gender	Mutations
1	GBM	70/M	IDHwt - MGMT low methylation
2	GBM	66/F	IDHwt - MGMT methylated

Transparent Methods

Cell culture

The murine microglial cell line BV2 were a kind gift from Dr. Anirban Basu (National Brain Research Centre, Gurgaon). The cells were cultured in DMEM, high glucose medium, supplemented with 10% FBS and 1 % antibiotic antimycotic stabilized solution (Himedia). The cells were grown in 96-well plate or in chamber slides as required. They were incubated at 37°C with 5% CO_2 for 24 hours (Eppendorf-170 S, Incubator). The confluent microplate or chamber slides were then used for experiments.

Primary human microglia isolation

Ethical clearance for acquiring tissues was taken from the Institute ethics committees of Indian Institute of Technology Jodhpur and All India Institute of Medical Science (AIIMS) Jodhpur. Informed consent was acquired for the use of tissue samples for experiments from human participants. A protocol for isolating primary microglia from adult human brain tissues was developed (Agrawal et al., 2020). Brain tissue was transported to lab in artificial cerebrospinal fluid (acsf) (2mM – $CaCl_2$-$2H_2O$, 10mM – Glucose, 3mM – KCl, 26mM – $NaHCO_3$, 2.5mM – NaH_2PO_4, 1mM – $MgCl_2$-$6H_2O$, 202mM – Sucrose) on ice. Tissue was washed for 5 minutes with acsf and then 5 minutes with PBS. Tissue was minced into small pieces and was incubated in 10ml trypsin for 25 minutes at 37°C. 10 ml media (DMEM/F12 with glutamine, 1% penicillin-streptomycin, 20% L929 supernatant, 10% FBS) was added and tissue was centrifuged at 2000xg for 10 minutes at 4°C. Supernatant was removed and the pellet was dissolved in media, plated and incubated at 37°C with 5% CO_2. On the 2nd day, considering the processing day as day 0, supernatant from the flask was collected and centrifuged at 1466xg for 4 minutes at 4°C. Supernatant was discarded and the pellet was plated in a fresh flask. Fresh media was added to the day 0 flask. Media of both flasks were changed again on the fourth and sixth day. The population of microglial cell were confirmed by staining them with *Ricinus communis* agglutinin-1 (RCA-1) lectin (Vector labs, FL-1081) (Jha et al., 2010). RCA stained cells were counted by blinded observers.

MTT assay

10,000 BV2 microglia cell were seeded per well in a 96 well plate. Cells were pretreated with either 10mM NAC for 3 hours or 10µM Cytochalasin D (CytoD) for 20 minutes and were incubated at 37°C with 5% CO_2. After pretreatment cells were treated with 250µM, 500µM, 750µM, 1mM of DA for 24 hours. DA containing media was removed carefully from the microplate. 100µl of fresh serum free media and 10µl of MTT solution (Sigma) was added to each well. The plate was kept in incubator (Model 170S, Eppendorf) at 37°C with 5% CO_2 in dark for 2 hours. After incubation, 100µl of acidic isopropanol solution was added to each well and mixed thoroughly using pipette. Absorbance at 570nm was measured using a multi-mode microplate reader (Synergy H1 Hybrid, Biotek Instruments Inc).

Immunocytochemistry

15,000 BV2 microglia cell seeded in each well of 2 well culture slides. Cells were pretreated with either 10mM NAC for 3 hours or 10µM CytoD for 20 minutes and were treated with mentioned concentration of DA or 24 hours. After treatment, cells were washed twice with 1X PBS for 5 minutes and were fixed for 10 minutes with 4% PFA. BV2 microglia cell were washed again twice and mounted with Fluoroshield with DAPI (Sigma-F6057). 15,000 primary adult human microglia cells were seeded in 2 well culture slides and treated with 2.5µM DA, LPS or 25nM PMA for 12 hours. 15,000 BV2 microglia cell were seeded in 2 well culture slides and treated with 250µM DA for 24 hours. After treatment, cells were washed twice with 1X PBS for 5 minutes and were fixed for 10 minutes with 4% PFA. Cells were washed again with 1X PBS and permeabilized with 0.1% TritonX-PBS for 15 minutes at room temperature. Further cells were blocked with 5% FBS in 0.1% TritonX-PBS for 1 hour in humidified chamber at 4°C and stained overnight in humidified chamber at 4°C with 1:1500 dilution of Anti-DNA/Histone H1 primary antibody (Merck, MAB3864) for primary cells and with 1:250 dilution of anti-Neutrophil Myeloperoxidase antibody (Sigma-Aldrich, N5787) for BV2 cells. After primary incubation, cells were washed and incubated for 1 hour with 1:500 dilution of anti-mouse or 1:1000 dilution of anti-rabbit secondary antibody. Cells were further washed and mounted with Fluoroshield with DAPI (Sigma-F6057). Images were taken using a fluorescence microscope (Leica Systems). Bright field images at 20X and 40X were taken on Nikon or Leica Microscope. Images were analyzed using ImageJ (Schneider et al., 2012).

Immunohistochemistry

We used 5-µm sections embedded in paraffin that were deparaffinized and rehydrated through alcohols (Jha et al., 2010). The paraffin embedded paraformaldehyde fixed glioma (grade 4, Glioblastoma) and normal brain tissue were obtained with approval from the Internal Review Board and the Ethics Committees of AIIMS, Jodhpur and Tata Memorial Cancer Hospitals. Informed consent was acquired for the use of tissue samples for experiments from human participants. We have performed all experiments in accordance with the ethical guidelines and regulations of All India Institute of Medical Sciences Jodhpur and Indian Institute of Technology Jodhpur. For the detection of microglia, tissues were stained with 1:500 *Ricinus communis agglutinin-1* (RCA-1) lectin (Vector labs, FL-1081) (Jha et al., 2010). Glioma (paraformaldehyde fixed paraffin embedded grade IV glioblastoma) and normal brain (paraformaldehyde fixed paraffin embedded) tissue sections were stained for DNA/Histone H1 using 1:300 of anti- DNA/Histone H1 antibody (Merck) primary antibody and 1:500 anti-mouse secondary antibody. Nuclei were stained blue with DAPI. Immunofluorescence was observed using fluorescence microscope (Leica Systems) and analyzed using ImageJ (Schneider et al., 2012).

Quantification of extracellular traps in tissues

5-µm embedded paraffin sections of GBM and cerebrum were stained as described in immunohistochemistry section. The number of punctate structure with RCA, for microglia, and DNA/Histone H1, for ETs, overlap were quantified by the algorithm developed by us. The average of the quantified value was represented on the graph. Error bars represent standard error. The data is representative of two experiments.

Quantification of extracellular traps in culture supernatant

The ETs in supernatant was quantified by measuring the fluorescence of digested traps (Robledo-Avila et al., 2018, Yoo et al., 2014, Joshi et al., 2013). 2,00,000 cells were seeded in 6 well plate. Cells were treated with 250µM of dopamine and were incubated at 37°C with 5% CO_2 for 24 hours. Following incubation 10U/ml DNase I Solution (Himedia) was added to the wells and the plate was incubated at room temperature for 15 minutes. 5mM EDTA was added to the wells to stop the reaction. Supernatant was collected and centrifuged at 300g at room temperature. After

centrifugation supernatant was transferred to clean centrifuge tubes. 200µl of supernatant was added to wells in a 96 well plate in duplicates. 5µM SYTOX™ Green Nucleic Acid Stain (Invitrogen) was added to the wells and the plate was incubated in dark for 15 minutes. The fluorescence was measured at excitation/emission = 485/530.

Extracellular traps functional assay

15,000 BV2 microglia cell seeded in 2 well chamber slides. After pretreatment with NAC or CytoD, as mentioned above, cells were treated with 250µM DA and incubated at 37°C with 5% CO_2. FITC tagged *E. coli* taken from Vybrant Phagocytosis Assay Kit (V-6694), was added after 3 hours of addition of DA. Cells were further incubated at 37°C with 5% CO_2 for 21 hours. Cells were washed twice with 1X PBS for 5 minutes and were fixed with 4% PFA. Then they were washed again twice with 1X PBS for 5 minutes and were mounted with Fluoroshield with DAPI. Images were taken using a fluorescence microscope (Leica Systems)

Detection of ROS

10,000 cells were seeded in 96 well microtiter plate and were incubated overnight at 37°C with 5% CO_2. Cells were treated with 20µM of 2′, 7′-Dichlorofluorescin diacetate (D6883 Sigma) for 30 minutes. Media was removed and the cells were washed once with 1X PBS. 100µl media was added to each well and cells were treated with 10mM NAC for 3 hours. Following this treatment cells were treated with 250µM DA for 24 hours. Fluorescence intensity indicating ROS generation was measured with a Synergy H1 Hybrid Multi-Mode reader (BioTek) at excitation and emission wavelength of 485/535 nm.

Algorithm and code for quantification of extracellular traps in tissues

There are three primary chromatic colors of light present there in the digital cell images. Those are red (R), green (G) and blue (B). As we know, any digital color image consists of those three color channels and any other color is a combination of these three with different proportion (Koschan and Abidi, 2008, Gonzalez and Woods, 2018). We have utilized this basic property of digital color images while determining the

overlapping between different regions. We have extracted out the three different color channels from the color image and processed those separately to determine the overlapped regions. That is, we perform a thresholding operation on each of the R, G and B images separately and carried out intersection operations between them.

Say, *I* is the colored cell image under consideration. In the other words, it can be said that *I* is a matrix of size *MXNX3*. Now, after extracting out three color channels there will be three different images each of size *MXN*. Let those be denoted as I_R, I_G *and* I_B. Let we set three threshold values T_R, T_G *and* T_B to extract out the regions with higher values of these three colors in the three images. The thresholding operation on I_R is carried out according to the equation given below.

$$B_R = \begin{matrix} 1 \; if \; I_R > \; T_R \\ 0 \quad otherwise \end{matrix}$$

B_R is the binarized image that we receive after performing thresholding on I_R. Please note, the pixels with value '1' in B_R represents the pixels with higher red component present in it. Similarly, we can have two more binarized images from I_G *and* I_B as B_G *and* B_B with threholds T_G *and* T_B respectively.

To determine the overlapped regions between red and green regions we perform $B_R \cap B_G$. The intersected region will reflect the overlapped areas of red and green regions in the cell image. The same will be performed between $B_G \cap B_B$, and $B_R \cap B_B$ to determine the green-blue and red-blue overlapped regions.

Further, we have eliminated the noisy regions those were present in the intersected image. We have considered the small regions as noise and eliminated them. The small regions are chosen to be of 10% of size of the largest region that is present in the intersected image. The remaining regions will finally be labelled as the overlapped regions.

The code for quantification is as follows:

```
clear;

I1=imread('C:\Users\RISHABH\Documents\IHC-Glioma&Cerebrum-ASC-P3-CD11b-
quantificationImages\IHC-Glioma&Cerebrum-ASC-P3-CD11b-
quantificationImages\Cerebrum_CD11b&ASC\edited-Blue-35B&50C&RedGreen-
```

```
50B&40C\IHC-Glioma&Cerebrum-ASC-P3-CD11b-
quantificationImages\Cerebrum_CD11b&ASC\edited-Blue-35B&50C&RedGreen-
50B&40C/image0466.tif');

[xr yr]=find(I1(:,:,1)>100 & I1(:,:,2)>70 & I1(:,:,3)>70);

I2=uint8(zeros(size(I1)));

a1=size(xr)

for i=1:a1

I2(xr(i),yr(i),:)=255;

end


bw=im2bw(I2);

se = strel('sphere',5);

    dilatedBW = imclose(bw, se);

figure, imshow(I1)


%%%%%%%%%%%%%%%%%%%%%%%%%%%%%%%%%%%%%%%%%%
%%%%%%%%%%%%%%%

measurements=regionprops(dilatedBW,'Area');

      %a1=measurements.Area;

      areaIm=zeros(1,length(measurements));

      if length(measurements)>1

      for k = 1 : length(measurements)

   areaIm(k) = measurements(k).Area;

      end
```

```
       sz=floor(max(areaIm)/10);

       NewBW=bwareaopen(dilatedBW,sz);

      %imshow(NewBW);

%%%%%%%%%%%%%%%%%%%%%%%%%%%%%%%%%%%%%%%%%%%%%%%%%%%%%%%%%%%%%%%%%%%%%%%%%%%%%%%%%%%%%%%%%%%%%%%%%%%%%%%%%%%%%%%%%%%%%%%%%%%%%%%%%%%%%%%%%%%%%%%%%%%%%%%%%%%%%%%%%%%%%%%%%%%%%%%%%%%%%%

         stats = regionprops('table',NewBW,'Centroid', ...

                         'MajorAxisLength','MinorAxisLength');

         % Get centers and radii of the circles

         centers = stats.Centroid;

         c1=size(centers);

         diameters = mean([stats.MajorAxisLength stats.MinorAxisLength],2);

         radii = diameters/2;

         c11=c1(1);

         if c11<1

             c11=0;

         end

wrt1=sprintf('Regions with Red Green Blue Overlapping = %d', c11);

title(wrt1)

         % Plot the circles

         hold on

         viscircles(centers,radii);
```

```
          hold off
wrt2=sprintf('RedGreenBlueOverlap.tif');
imwrite(I1,wrt2);
        else
            print('No Overlapping RedGreenBlue');
        end
[xg yg]=find(I1(:,:,1)>100 & I1(:,:,2)<50 & I1(:,:,3)>70);
I2=uint8(zeros(size(I1)));
a1=size(xg);
for i=1:a1
I2(xg(i),yg(i),:)=255;
end
bw=im2bw(I2);


se = strel('sphere',5);
     dilatedBW = imclose(bw, se);


%%%%%%%%%%%%%%%%%%%%%%%%%%%%%%%%%%%%%%%%%%%%%%%%%%%%%%%%%%%%%%%%%%%%%%%%
measurements=regionprops(dilatedBW,'Area');
        %a1=measurements.Area;
```

```
areaIm=zeros(1,length(measurements));
if length(measurements)>1
for k = 1 : length(measurements)
areaIm(k) = measurements(k).Area;
end
sz=floor(max(areaIm)/10);
NewBW=bwareaopen(dilatedBW,sz);
%imshow(NewBW);
%%%%%%%%%%%%%%%%%%%%%%%%%%%%%%%%%%%%%%%%%%%%%%%%%%%%%%%%%%%%%%%%%%%%

stats = regionprops('table',NewBW,'Centroid', ...
                'MajorAxisLength','MinorAxisLength');

figure, imshow(I1)

%stats = regionprops('table',dilatedBW,'Centroid', ...
                %'MajorAxisLength','MinorAxisLength');

% Get centers and radii of the circles
centers = stats.Centroid;
c1=size(centers);
c11=c1(1);
```

```
        if c11<1
            c11=0;
        end
        diameters = mean([stats.MajorAxisLength stats.MinorAxisLength],2);
        radii = diameters/2;
        wrt1=sprintf('Regions with Red Blue Overlapping = %d', c11);
        title(wrt1)
        % Plot the circles
        hold on
        viscircles(centers,radii);
        hold off
 else
          print('No Overlapping RedBlue');
       end
        %wrt2=sprintf('RedBlueOverlap.tif');
%imwrite(I1,wrt2);

[xg yg]=find(I1(:,:,1)<50 & I1(:,:,2)>70 & I1(:,:,3)>70);
I2=uint8(zeros(size(I1)));
a1=size(xg);
for i=1:a1
I2(xg(i),yg(i),:)=255;
end
```

```
bw=im2bw(I2);
se = strel('sphere',5);
    dilatedBW = imclose(bw, se);


%%%%%%%%%%%%%%%%%%%%%%%%%%%%%%%%%%%%%%%%%%%%
%%%%%%%%%%%%%%%
measurements=regionprops(dilatedBW,'Area');
        %a1=measurements.Area;
        areaIm=zeros(1,length(measurements));
        if length(measurements)>1
        for k = 1 : length(measurements)
    areaIm(k) = measurements(k).Area;
        end
        sz=floor(max(areaIm)/10);
        NewBW=bwareaopen(dilatedBW,sz);
       %imshow(NewBW);
%%%%%%%%%%%%%%%%%%%%%%%%%%%%%%%%%%%%%%%%%%%%
%%%%%%%%%%%%%%


          stats = regionprops('table',NewBW,'Centroid', ...
                           'MajorAxisLength','MinorAxisLength');


figure, imshow(I1)
```

```
        % Get centers and radii of the circles
        centers = stats.Centroid;
        c1=size(centers);
        c11=c1(1);
        if c11<1
            c11=0;
        end
        diameters = mean([stats.MajorAxisLength stats.MinorAxisLength],2);
        radii = diameters/2;
        wrt1=sprintf('Regions with Green Blue Overlapping = %d', c11);
        title(wrt1)
        % Plot the circles
        hold on
        viscircles(centers,radii);
        hold off
      end
[xg yg]=find(I1(:,:,1)>70 & I1(:,:,2)>50 & I1(:,:,3)<50);
I2=uint8(zeros(size(I1)));
a1=size(xg);
for i=1:a1
I2(xg(i),yg(i),:)=255;
```

```
end

bw=im2bw(I2);

se = strel('sphere',10);

     dilatedBW = imclose(bw, se);



%%%%%%%%%%%%%%%%%%%%%%%%%%%%%%%%%%%%%%%%%%%%%%%%%%%%%%%%%%%%%

measurements=regionprops(dilatedBW,'Area');

if length(measurements)>1

        %a1=measurements.Area;

        areaIm=zeros(1,length(measurements));

        for k = 1 : length(measurements)

    areaIm(k) = measurements(k).Area;

        end

        sz=floor(max(areaIm)/10);

        NewBW=bwareaopen(dilatedBW,sz);

       %imshow(NewBW);

%%%%%%%%%%%%%%%%%%%%%%%%%%%%%%%%%%%%%%%%%%%%%%%%%%%%%%%%%%%%


          stats = regionprops('table',NewBW,'Centroid', ...

                            'MajorAxisLength','MinorAxisLength');
```

```
figure, imshow(I1)



        % Get centers and radii of the circles

        centers = stats.Centroid;

        c1=size(centers);

        c11=c1(1);

        if c11<1

           c11=0;

        end

        diameters = mean([stats.MajorAxisLength stats.MinorAxisLength],2);

        radii = diameters/2;

        wrt1=sprintf('Regions with Red Green Overlapping = %d', c11);

        title(wrt1)

        % Plot the circles

        hold on

        viscircles(centers,radii);

        hold off

end
```

Supplemental References:

AGRAWAL, I., SAXENA, S., NAIR, P., JHA, D. & JHA, S. 2020. Obtaining Human Microglia from Adult Human Brain Tissue. *JoVE***,** e61438.

GONZALEZ, R. C. & WOODS, R. E. 2018. ***Digital Image Processing***, Pearson.

JHA, S., SRIVASTAVA, S. Y., BRICKEY, W. J., IOCCA, H., TOEWS, A., MORRISON, J. P., CHEN, V. S., GRIS, D., MATSUSHIMA, G. K. & TING, J. P. Y. 2010. The inflammasome sensor, NLRP3, regulates CNS inflammation and demyelination via caspase-1 and interleukin-18. *The Journal of neuroscience : the official journal of the Society for Neuroscience,* 30**,** 15811-15820.

JOSHI, M. B., LAD, A., BHARATH PRASAD, A. S., BALAKRISHNAN, A., RAMACHANDRA, L. & SATYAMOORTHY, K. 2013. High glucose modulates IL-6 mediated immune homeostasis through impeding neutrophil extracellular trap formation. *FEBS Letters,* 587**,** 2241-2246.

KOSCHAN, A. & ABIDI, M. 2008. ***Digital Color Image Processing***, Wiley.

ROBLEDO-AVILA, F. H., RUIZ-ROSADO, J. D. D., BROCKMAN, K. L., KOPP, B. T., AMER, A. O., MCCOY, K., BAKALETZ, L. O. & PARTIDA-SANCHEZ, S. 2018. Dysregulated Calcium Homeostasis in Cystic Fibrosis Neutrophils Leads to Deficient Antimicrobial Responses. *The Journal of Immunology,* 201**,** 2016.

SCHNEIDER, C. A., RASBAND, W. S. & ELICEIRI, K. W. 2012. NIH Image to ImageJ: 25 years of image analysis. *Nature methods,* 9**,** 671-675.

YOO, D.-G., FLOYD, M., WINN, M., MOSKOWITZ, S. M. & RADA, B. 2014. NET formation induced by Pseudomonas aeruginosa cystic fibrosis isolates measured as release of myeloperoxidase–DNA and neutrophil elastase–DNA complexes. *Immunology Letters,* 160**,** 186-194.